Electronic Supplementary Material (ESI) for Sustainable Energy & Fuels.

Supplementary Materials for

A systematic study of post-activation temperature dependence on photoelectrochemical water splitting of one-step synthesized FeOOH CF photoanodes with erratically loaded ZrO_2

Sarang Kim[a,§], Mahadik A. Mahadeo[a,§], Periyasamy Anushkkaran[a], Weon Sik Chae[b], Sun Hee Choi[c,*] and Jum Suk Jang[a,*]

[a] Division of Biotechnology, Safety, Environment and Life Science Institute, College of Environmental and Bioresource Sciences, Chonbuk National University, Iksan 570-752, Republic of Korea.

[b] Daegu Center, Korea Basic Science Institute, Daegu 41566, Republic of Korea.

[c] Pohang Accelerator Laboratory, POSTECH, Pohang 37673, Republic of Korea.

*Corresponding authors:

E-mail address: jangjs75@jbnu.ac.kr (Jum Suk Jang), shchoi@postech.ac.kr (S. H. Choi)

Tel.: +82 63 850 0846; fax: +82 63 850 0834.

§Authors with equal contributions.

Experimental for the preparation of the Ex-situ Zr-doped hematite photoanodes

0.4 g $FeCl_3.6H_2O$ and 0.85 g $NaNO_3$ were added into a 20 mL glass vial containing 10 mL deionized water with a pH of 1.5 and the cleaned FTO was kept in the vial. Then, the hydrothermal synthesis was conducted at 100 °C for 6 h. After the reaction, the as-grown β-FeOOH nanorod electrodes were systematically washed with DI water and immediately dried under nitrogen gas flow. Then, the as-grown β-FeOOH nanorod electrodes were immersed in the 4 % $ZrO(NO_3)_2$ ethanolic solution (4.1336 µL $ZrO(NO_3)_2$ in 10 mL ethanol) for 2 min. Subsequently, *ex-situ* Zr-doped FeOOH (Ex-Zr-FeOOH) thin films were heated for 10 min at different temperatures such as 650 °C, 700 °C, 750 °C, and 800 °C (heating rate 5 °C/min; average times taken to reach the temperatures are 130, 140, 150 and 160 min, respectively) and then quenched to room temperature. Further Ex-Zr-FeOOH converted into Ex-situ Zr-doped hematite and denoted as Ex-ZrQ650, Ex-ZrQ700, Ex-ZrQ750 and Ex-ZrQ800, respectively.

Table S1. Crystallite size of Zr-series samples annealed at different temperatures.

Samples	FWHM (110)	Crystallite size (nm)
ZrQ450	0.47	19
ZrQ550	0.45	20
ZrQ650	0.34	26
ZrQ700	0.28	31
ZrQ750	0.26	34
ZrQ800	0.25	35

Table S2. The atomic percentage of the elements from XPS for ZrO_2-FeOOH CF, ZrQ650, ZrQ700, ZrQ750, and ZrQ800 photoanodes respectively.

Samples	Zr (%)	Fe (%)	O (%)	Sn (%)
ZrO_2-FeOOH CF	7.20	21.13	71.67	0.00
ZrQ650	7.26	24.27	68.32	0.15
ZrQ700	5.95	27.54	66.36	0.14
ZrQ750	5.29	28.39	66.18	0.14
ZrQ800	4.88	29.38	65.61	0.12

Table S3. Structural parameters calculated from Fe K-edge EXAFS fits for ZrQ750 and EtQ750 photoanodes.

Samples	R_1 (Å)[a]	R_2 (Å)[b]	σ^2 (Å^2)[c]	R-factor[d]
ZrQ750	1.890	2.055	0.0037	0.0009
EtQ750	1.953	2.125	0.0040	0.0003
Fe_2O_3 ref*	1.957	2.128	0.0047	0.0002

[a,b]Fe-O bond distance (uncertainty < 0.005), [c]Debye-Waller factor (uncertainty < 0.001),
[d]a sum-of-squares measure of the fractional misfit.
*bulk α-Fe_2O_3 in powder

Table S4. Comparative photocurrent density results of hematite photoanodes prepared by different synthetic methods with low-temperature activation.

In situ elemental doping	Heat-treatment condition	Synthesis Method	Electrolyte	J_{ph} (mA/cm^2)	Ref.
Ti doped hematite	at 550˚C for 2 h & 650 ˚C for 15 min	Hydrothermal	1M NaOH	0.7 (1.4 V vs. RHE)	[1]
Ti doped hematite	at 550 °C for 2 h	Electrospray deposition	1M NaOH	1.09 (1.8 V vs. RHE)	[2]
Sn doped hematite (ex-situ doping)	at 550 °C for 2 h & 750 ˚C for 20 min	Hydrothermal Drop-coating	1M NaOH	0.94 (1.23 V vs. RHE)	[3]
Ta doped hematite	at 750 °C for 30min	Hydrothermal	0.5 M Na_2SO_4	0.53 (1.0 V vs. RHE)	[4]
Sn doped hematite	at 400°C for 4 h & 500°C for 0.5 h	Hydrothermal	1M NaOH	0.45 (1.23 V vs. RHE)	[5]
ZrO_2-Fe_2O_3 CF	**at 700 °C for 10 min at 750 °C for 10 min**	**Hydrothermal with dilution**	**1M NaOH**	**1.17 1.43 (1.23 V vs. RHE)**	**This study**

Table S5. Electron transport time results of the IMPS response for PQ800, ZrQ700, ZrQ750 and ZrQ800 at 1.23 V *vs.* RHE.

Samples	Frequency (Hz)	Electron transport time (ms)
PQ800	335	0.475
ZrQ700	355	0.449
ZrQ750	422	0.377
ZrQ800	502	0.317

Table S6. PL lifetime parameters of the hematite photocatalysts prepared from different synthetic conditions.

Sample	A_1 (%)	τ_1 (ns)	A_2 (%)	τ_2 (ns)	A_3 (%)	τ_3 (ns)	$<\tau>$ [a] (ns)
PQ800	99.2	0.24	0.8	2.8	-	-	0.47
EtQ800	99.2	0.22	0.8	6.5	-	-	1.39
ZrQ800	98.9	0.21	0.9	3.4	0.2	64	23

[a] The average lifetime ($<\tau>$) is defined by $<\tau>=\sum_i A_i\tau_i^2 / \sum_i A_i\tau_i$.[6]

Table S7. EIS fitting parameters obtained by fitting the experimental data of PQ750, EtQ750, and ZrQ750 photoanodes.

Samples/ Parameters	R_S (Ω)	R_{CT1} (Ω)	R_{CT2} (Ω)	CPE1 (F)	CPE2 (F)
PQ750	26.76	300	331.2	2.63×10^{-4}	1.46×10^{-5}
EtQ750	18.91	564	789	1.40×10^{-4}	1.24×10^{-5}
ZrQ750	27.58	110	174.2	9.83×10^{-4}	1.89×10^{-5}

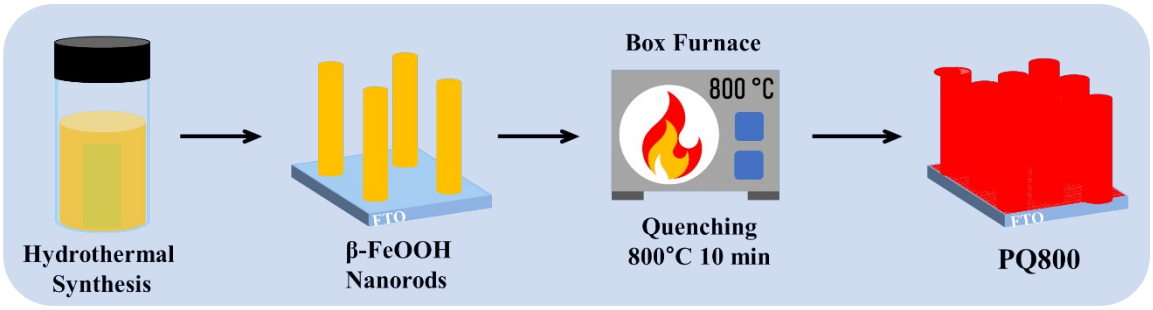

Fig. S1. Reference experiment of synthesis of PQ800 synthesized by conventional hydrothermal approach.

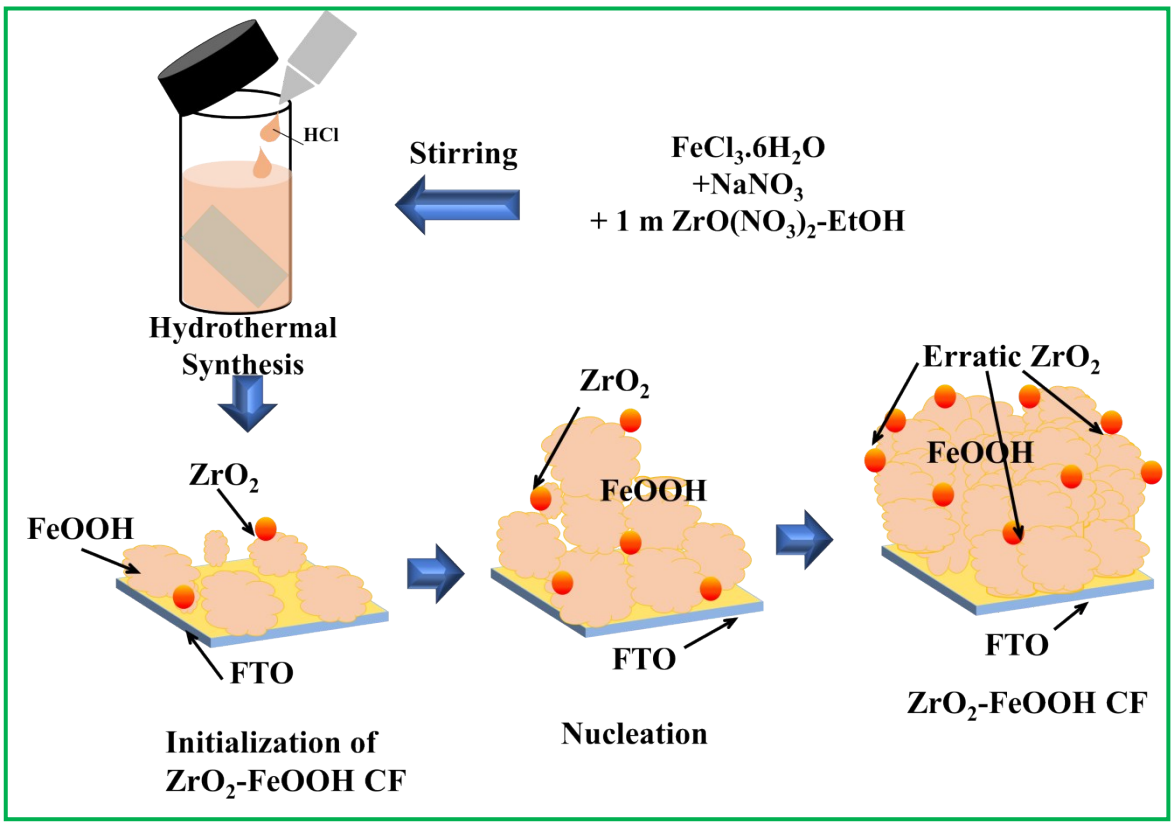

Fig. S2. Formation mechanism of the ZrO_2-FeOOH CF during the hydrothermal synthesis.

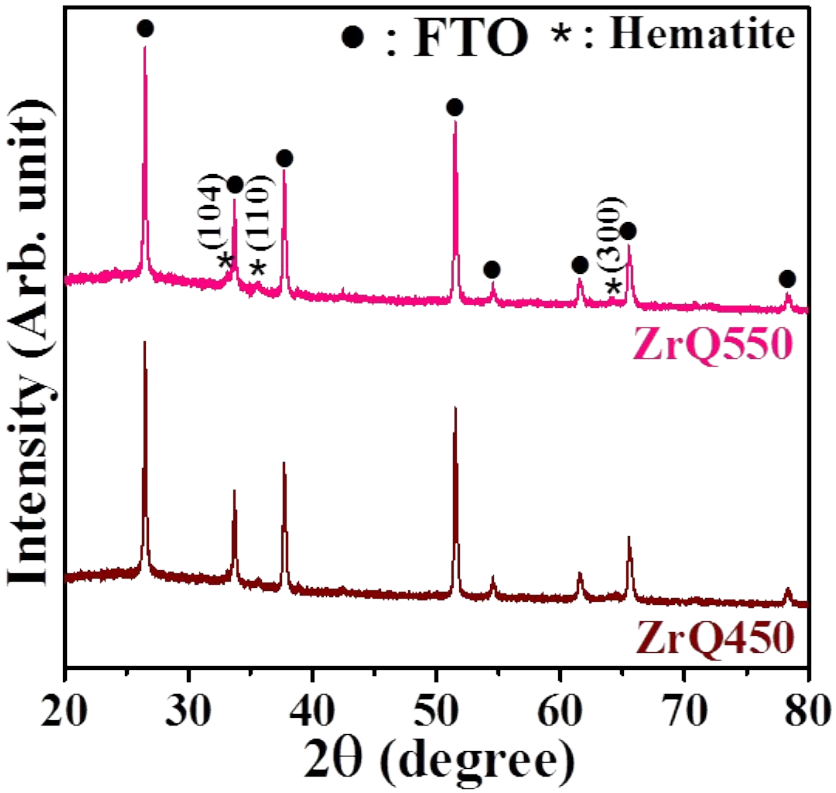

Fig. S3. (a) XRD patterns of ZrQ450, and ZrQ550 photoanodes. The '*' denotes the hematite (α-Fe_2O_3) and '●' denotes the FTO substrate (JCPDS 41–1445).

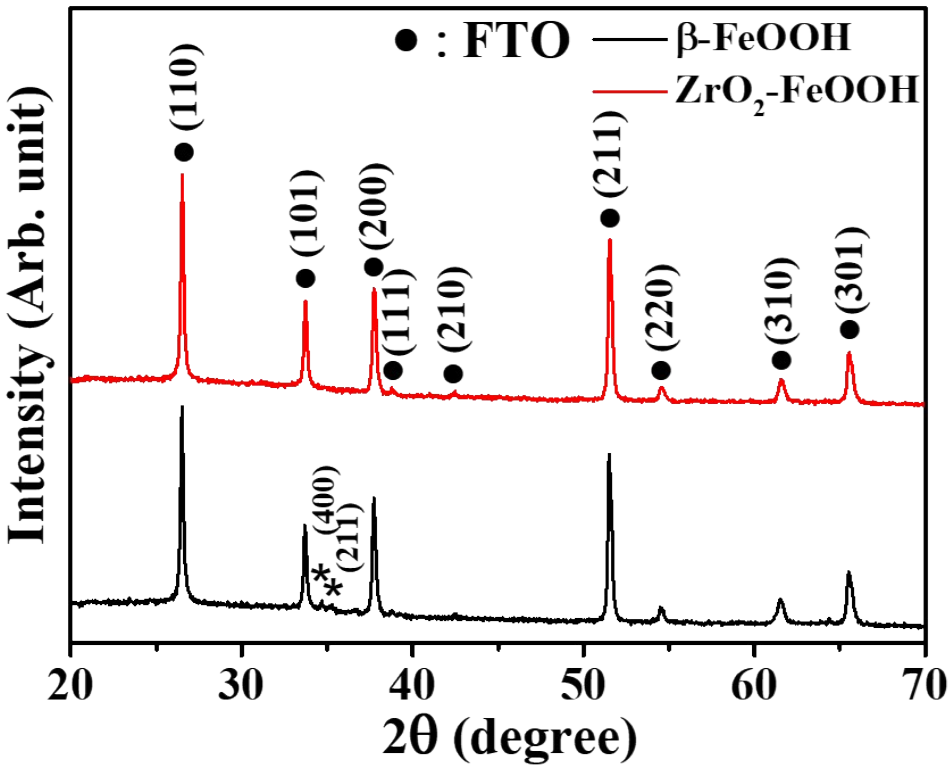

Fig. S4. XRD peaks of β-FeOOH and ZrO_2-FeOOH CF samples.

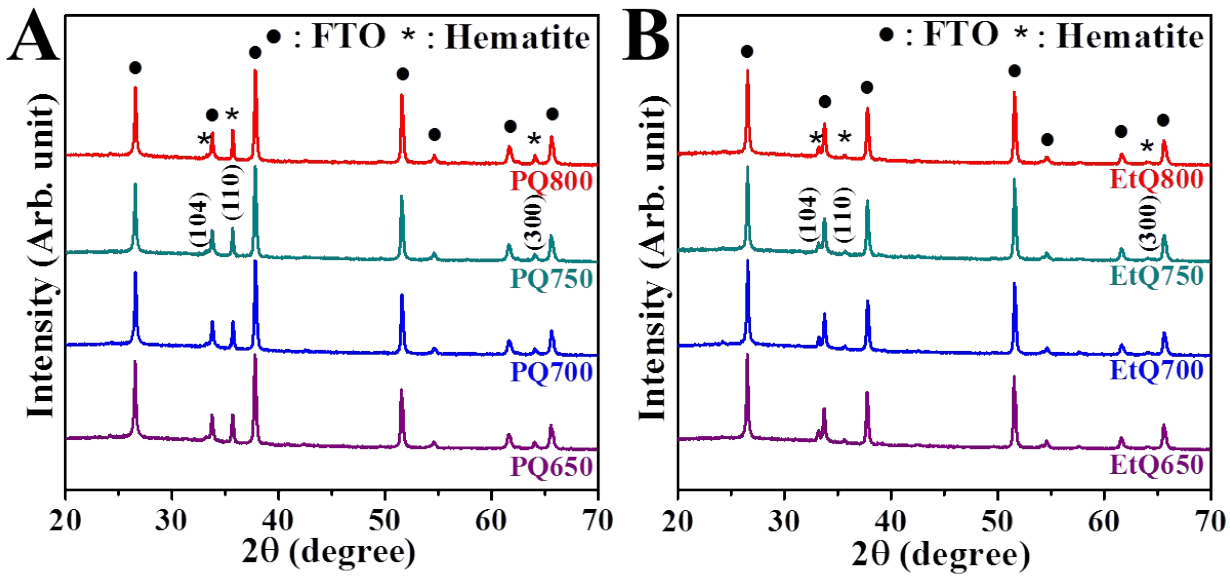

Fig. S5. X-ray diffraction patterns of (A) P-series samples and (B) Et-series samples, respectively.

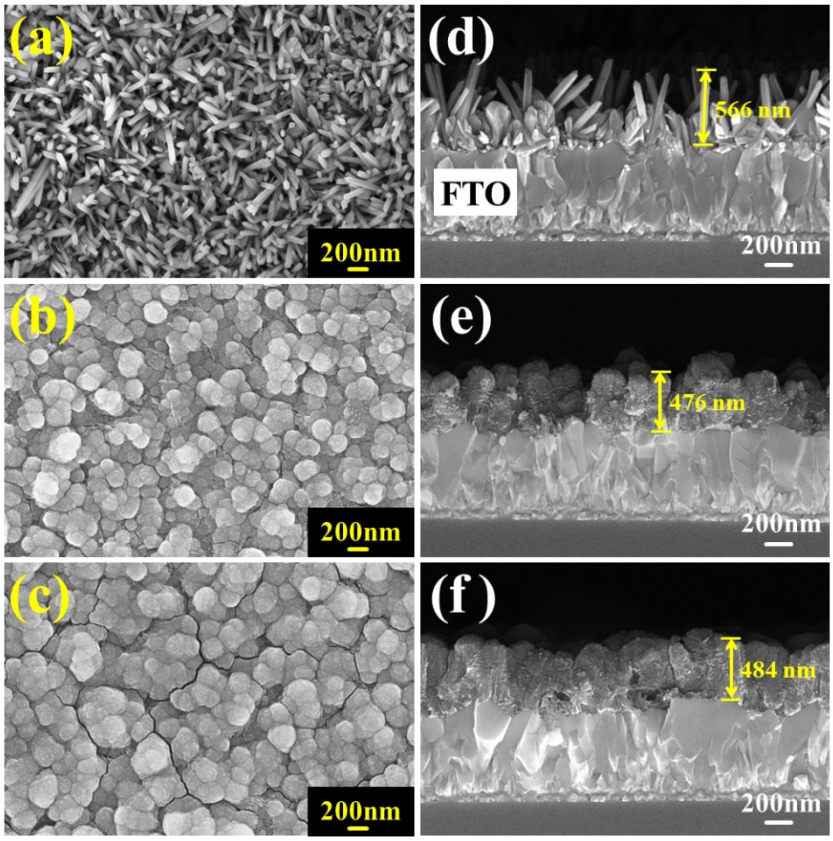

Fig. S6. FE-SEM, top view and cross-view images of (a-d) β–FeOOH, (b-e) ZrO_2–FeOOH CF, and (c-f) Et–FeOOH samples.

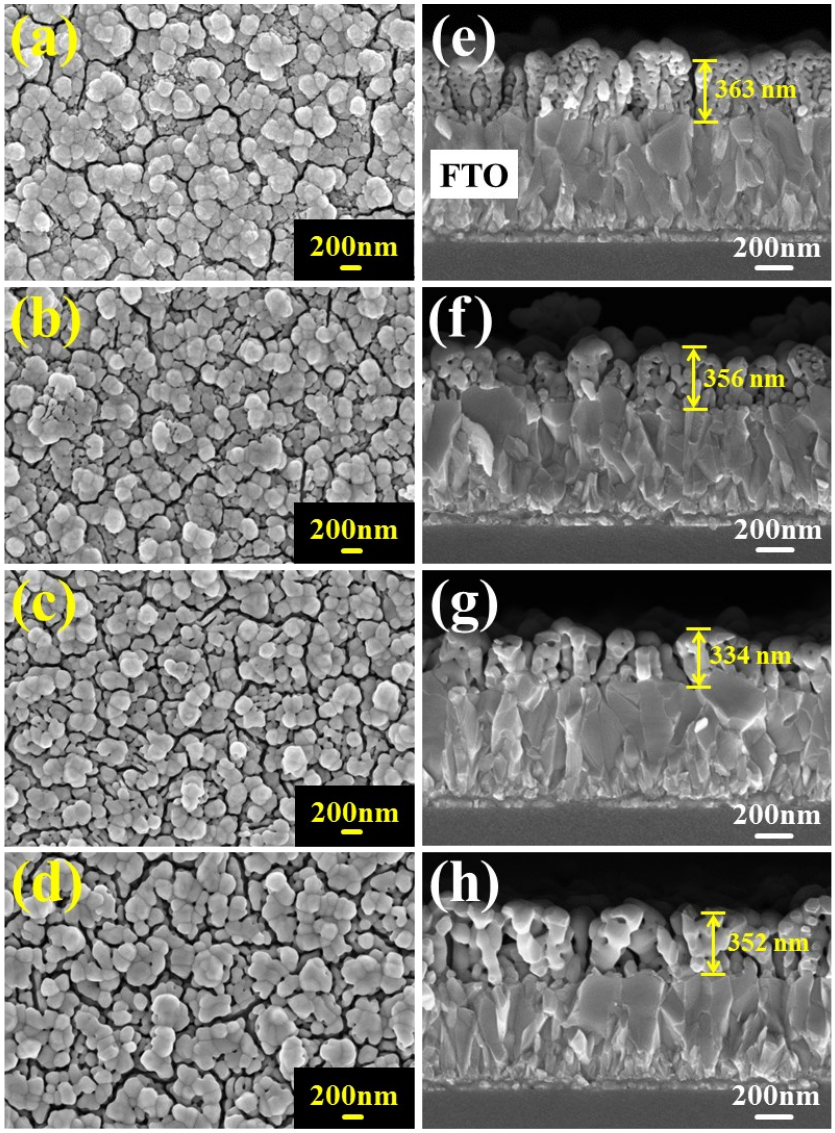

Fig. S7. FE-SEM, top view and cross-sectional images of Et-series samples (a-e) EtQ650, (b-f) EtQ700, (c-g) EtQ750 and (d-h) EtQ800, respectively.

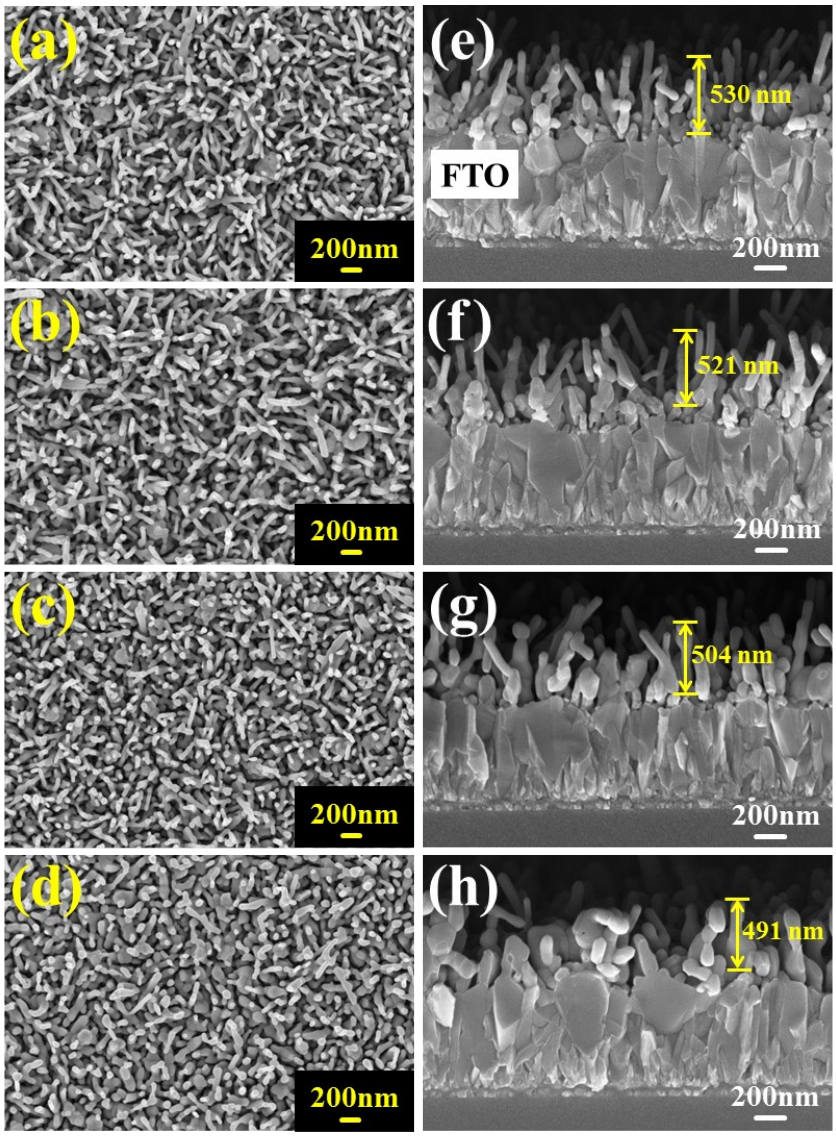

Fig. S8. FE-SEM, top view and cross-sectional images of P-series samples (a-e) PQ650, (b-f) PQ700, (c-g) PQ750 and (d-h) PQ800, respectively.

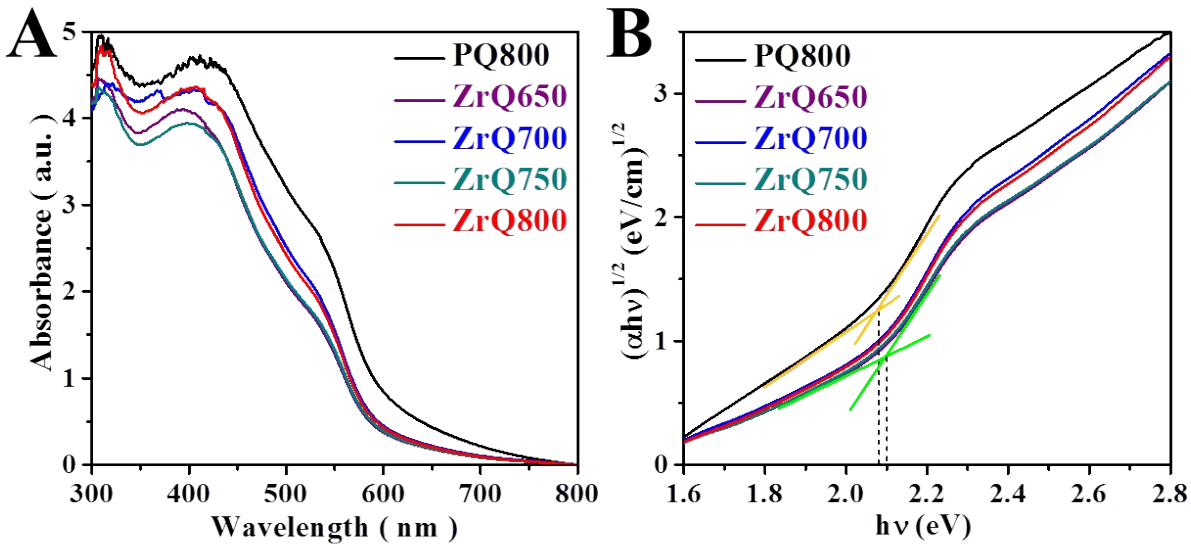

Fig. S9. (A) UV–vis absorbance spectra and (B) Tauc plots for the indirect bandgap of PQ800 and Zr-series photoanodes.

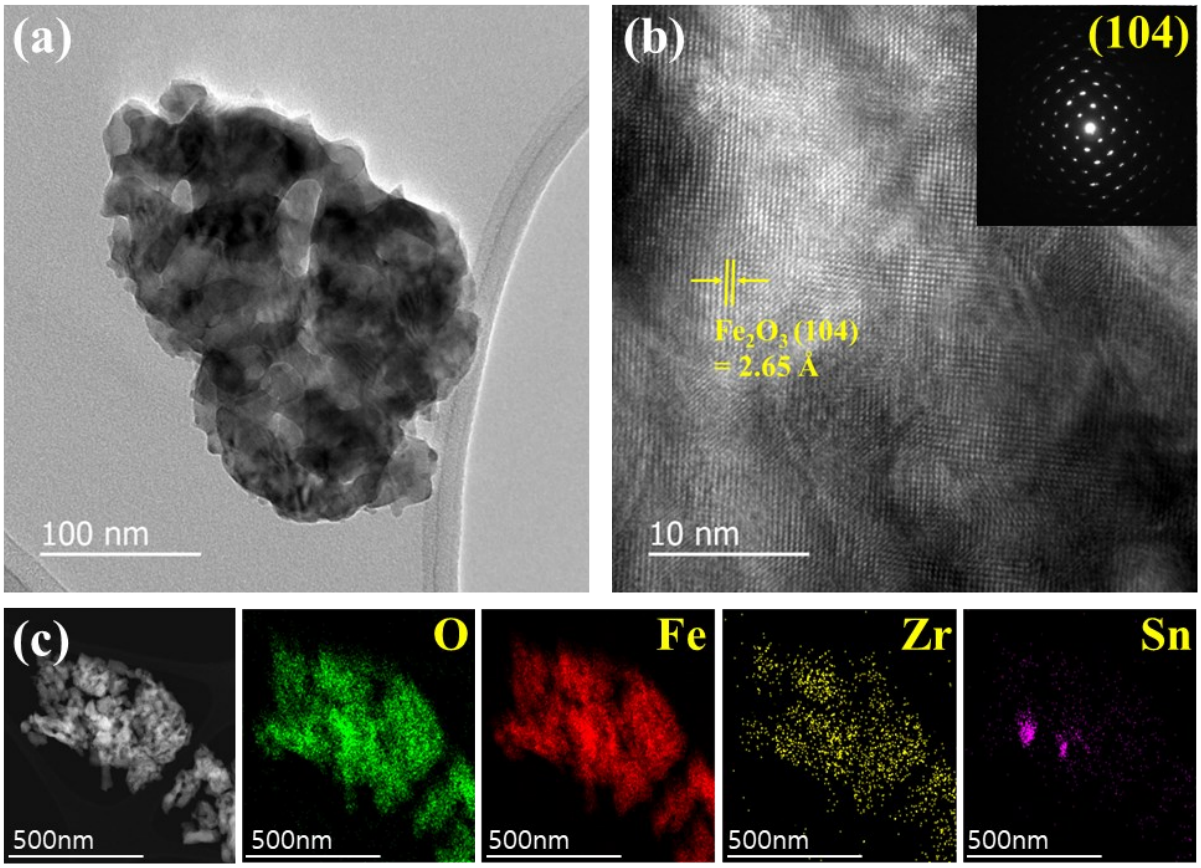

Fig. S10. (a) Low magnification TEM images, (b) HR-TEM images, (c) ADF-STEM images and EDS elemental mapping images of ZrQ750. Insets: FFT pattern of HR-TEM images.

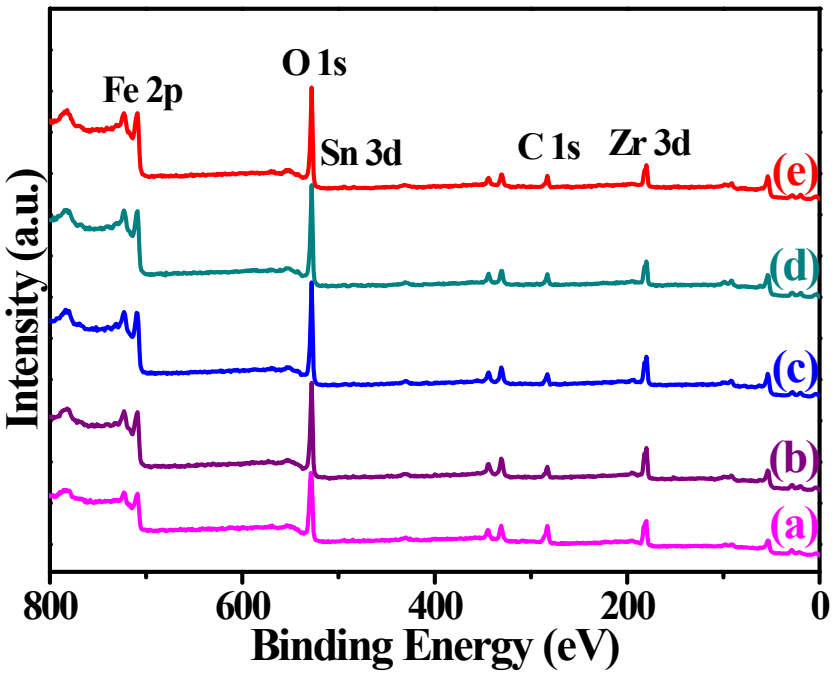

Fig. S11. XPS survey scan of (a) ZrO_2–FeOOH CF, (b) ZrQ650, (c) ZrQ700, (d) ZrQ750 and (e) ZrQ800 photoanodes.

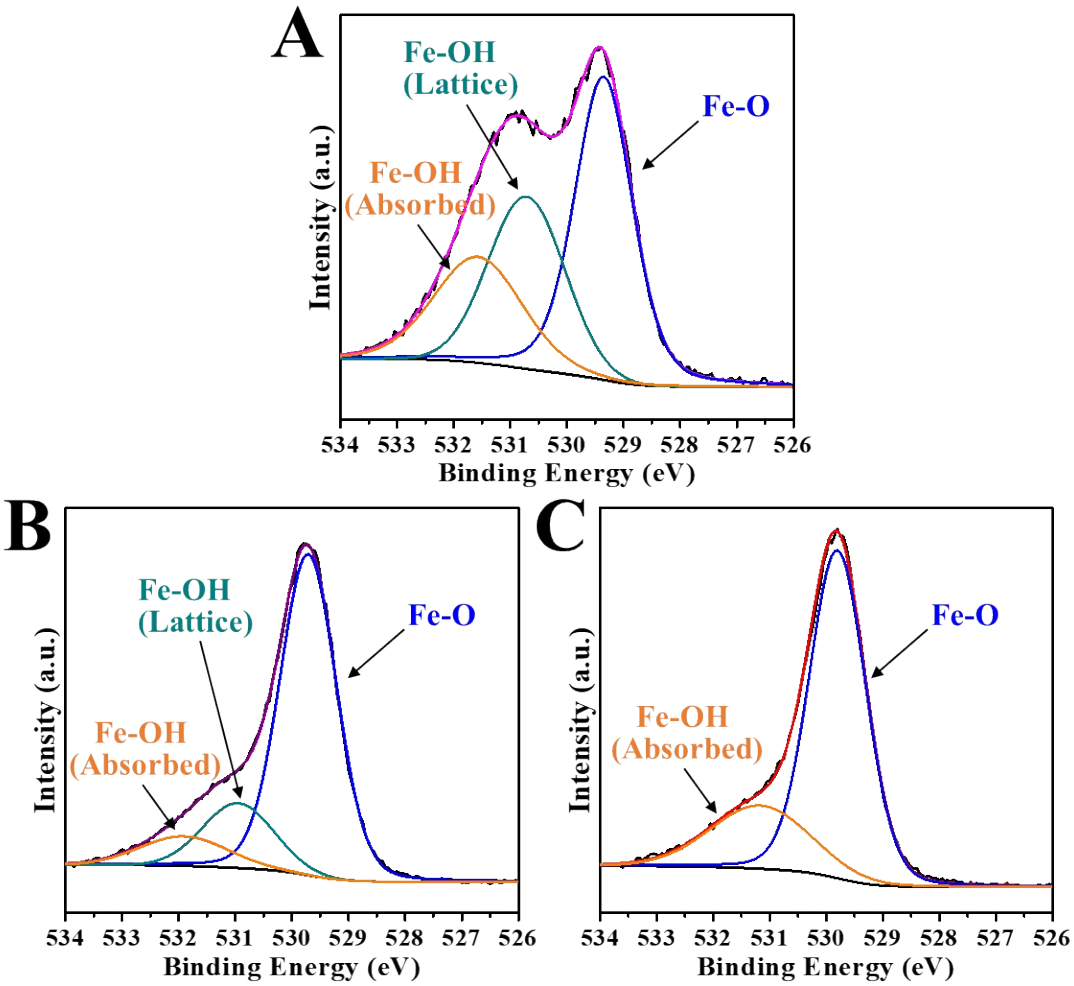

Fig. S12. Deconvolution of the O1s spectra for (A) ZrO_2–FeOOH CF, (B) ZrQ650, and (C) ZrQ800 photoanodes.

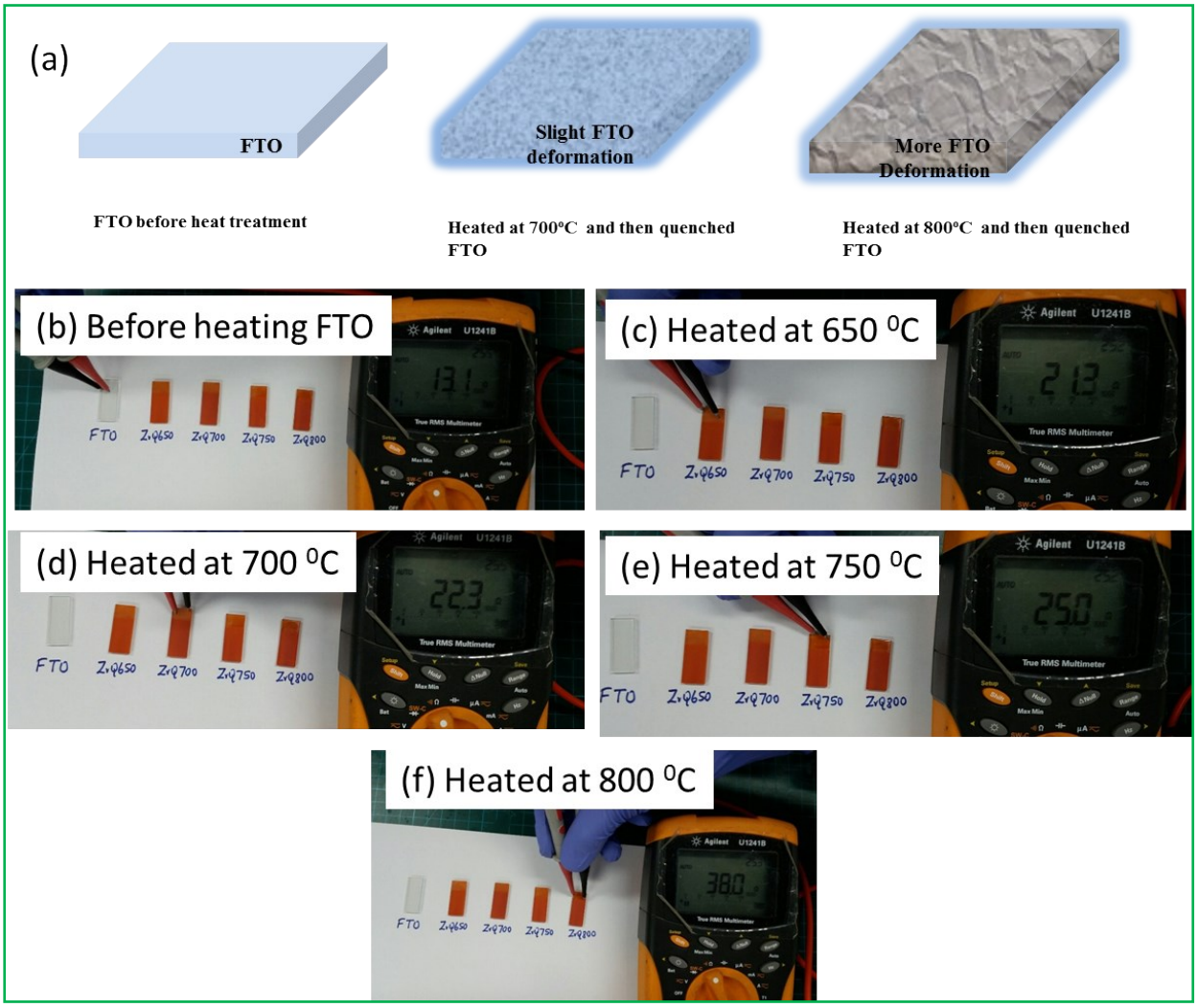

Figure S13. (a) Schematics of FTO samples with and without quenched at different temperatures, (b-f) actual photographs of the resistance measurements of FTO with a multimeter set on resistance mode for Zr-series samples.

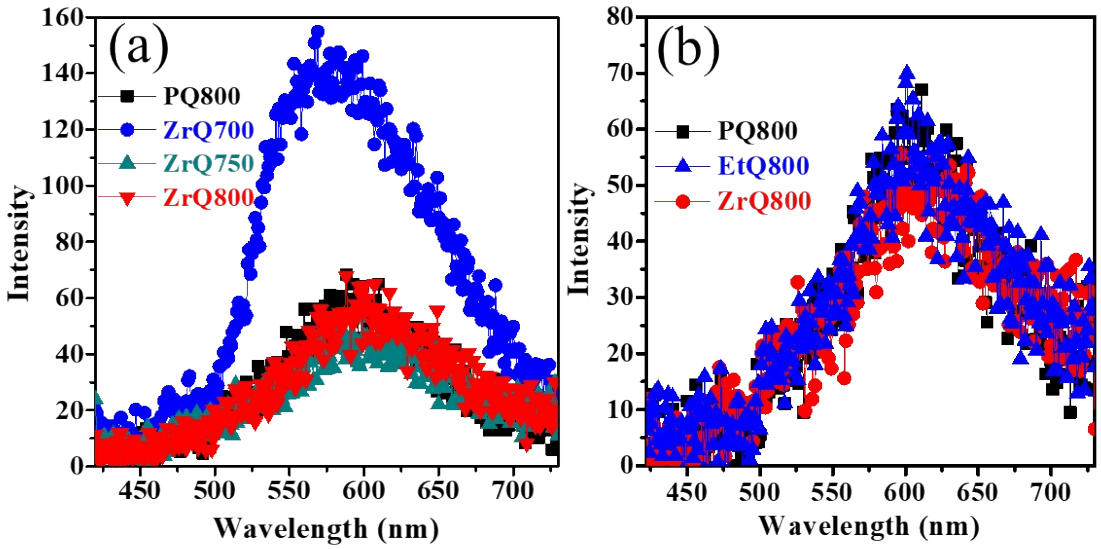

Fig. S14. (a) Photoluminescence spectra of the PQ800 (square), ZrQ700 (circle), ZrQ750 (up triangle), and ZrQ800 (down triangle) materials. (b) The photoluminescence spectra of the PQ800 (square), EtQ800 (up triangle), and ZrQ800 (circle) materials set are additionally displayed for clear comparison. A 470 nm laser line was used for this PL study.

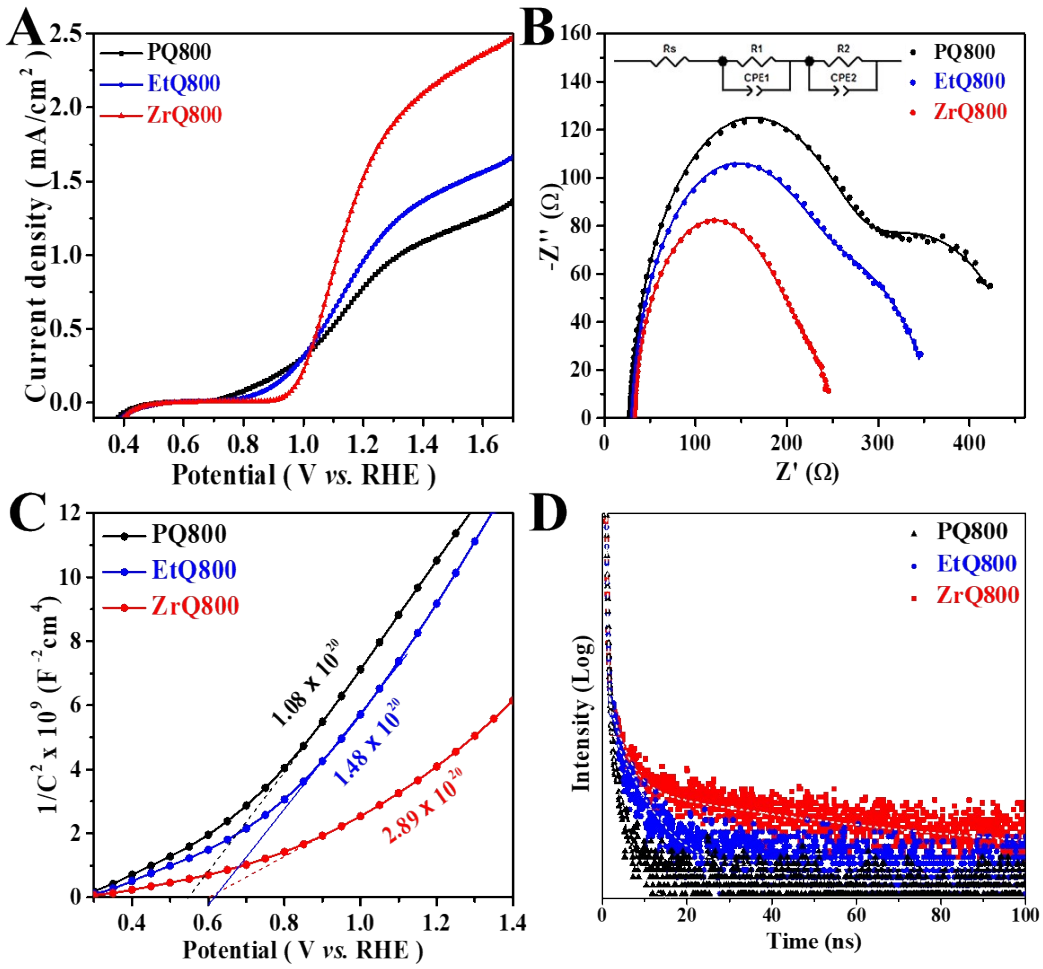

Fig. S15. (A) Photocurrent density–potential curves under light (solid lines) and dark (dashed lines) conditions, (B) Nyquist plots measured at 1.23 V *vs*. RHE with an equivalent circuit, (C) Mott–Schottky plots that were measured under a dark condition (D) Time-resolved PL decays of the PQ800, EtQ800, and ZrQ800 photoanodes. The overlapped dotted line is the fitted line.

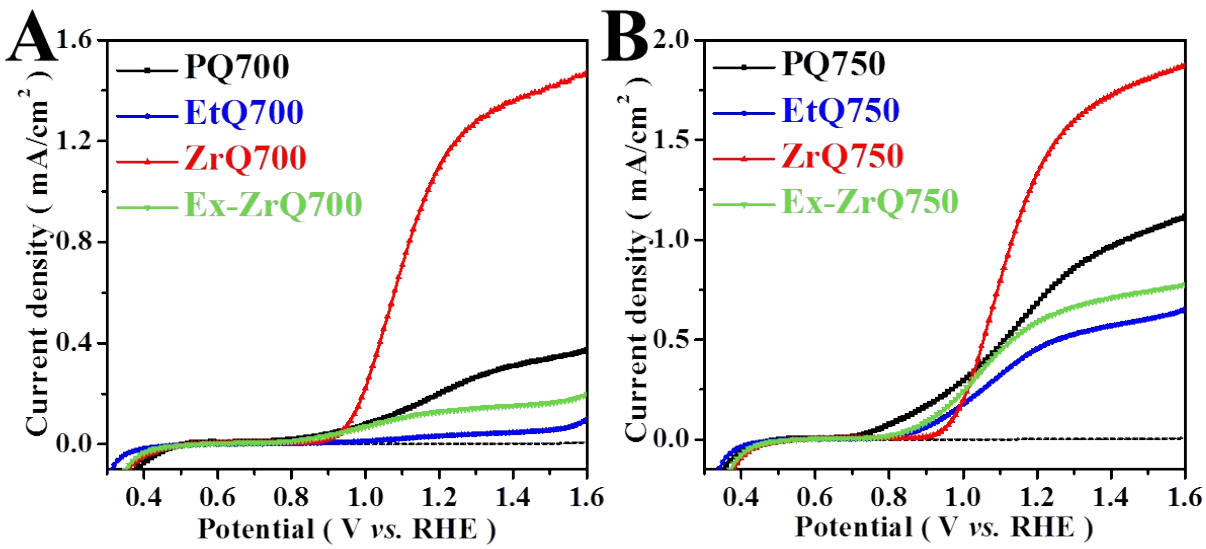

Fig. S16. Photocurrent density–potential curves under illumination (solid lines) and dark (dashed lines) conditions for (A) 700-series and (B) 750-series photoanodes.

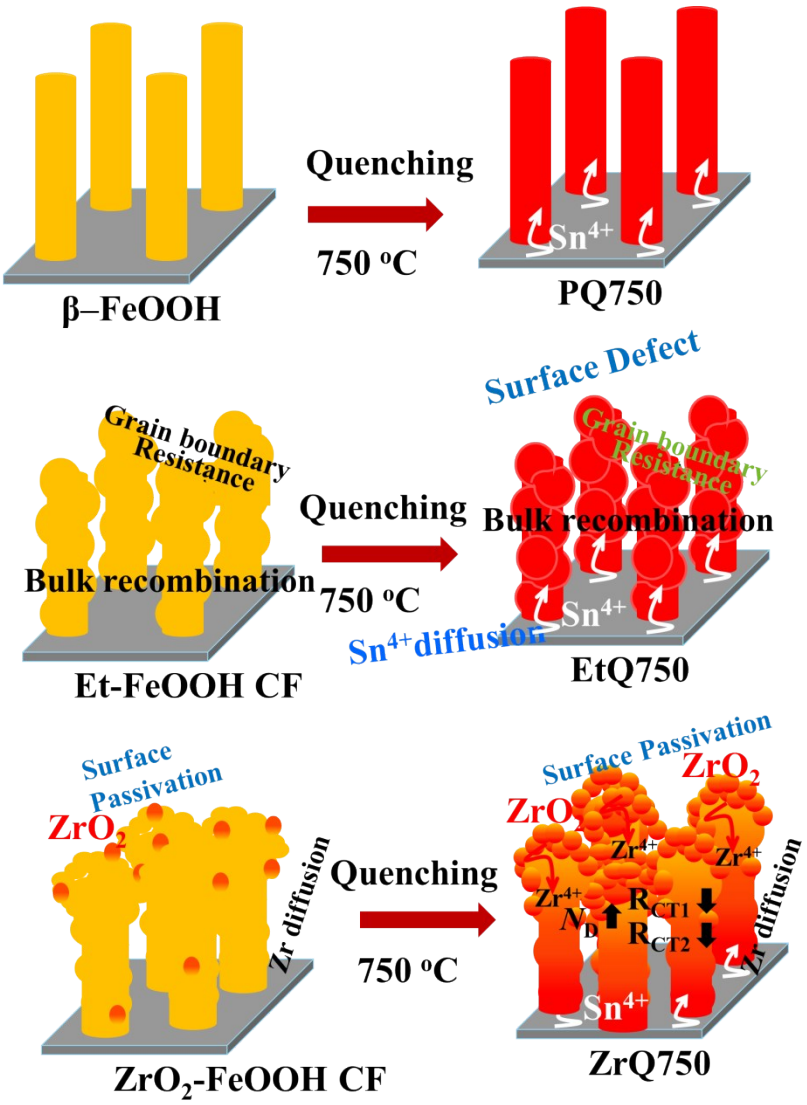

Fig. S17. Propose mechanism of erratic ZrO_2 formation during hydrothermal and Zr diffusion during the transformation of ZrO_2-FeOOH CF to ZrO_2- Fe_2O_3 CF.

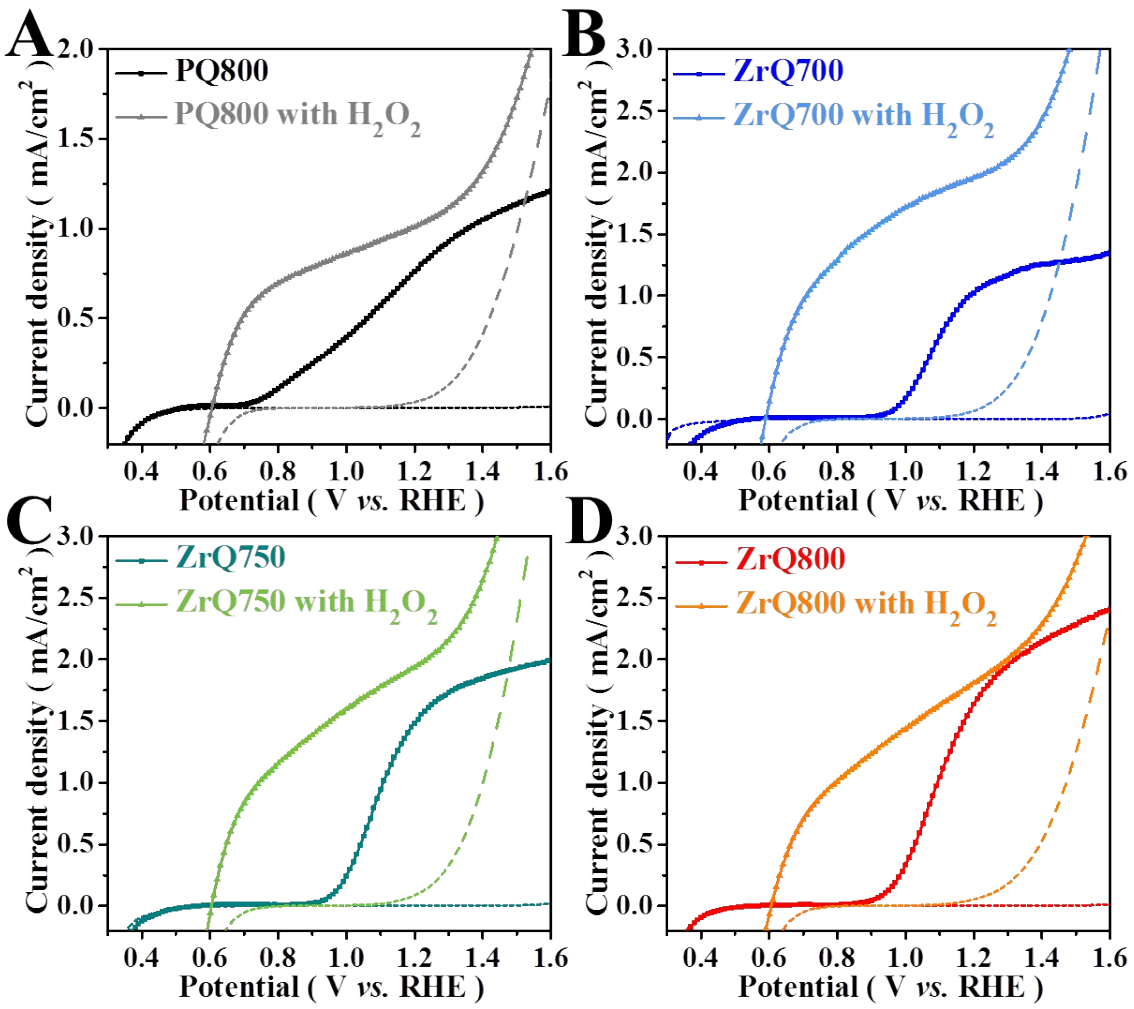

Fig. S18. Photocurrent density–potential curves under illumination (solid lines) and dark (dashed lines) conditions for (A) PQ800, (B) ZrQ700, (C) ZrQ750, and (D) ZrQ800 photoanodes with /without 0.5 M H_2O_2 as a hole scavenger.

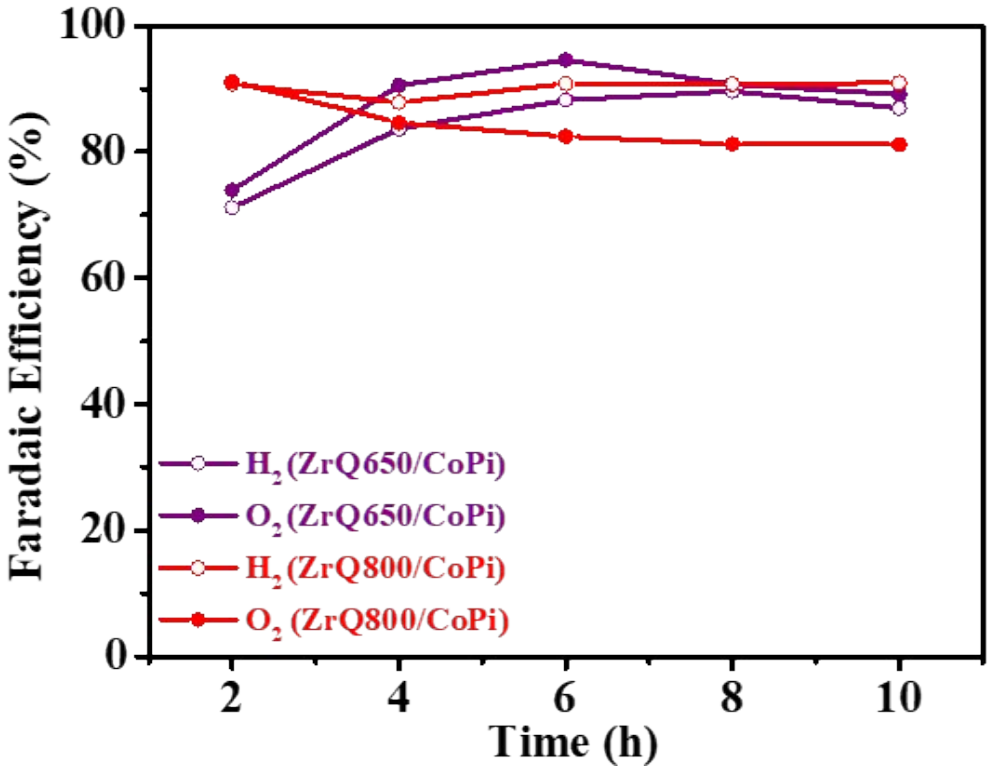

Fig. S19. Faradaic efficiency for the ZrQ650/CoPi and ZrQ800/CoPi photoanodes at an applied voltage of 1.23 V *vs.* RHE.

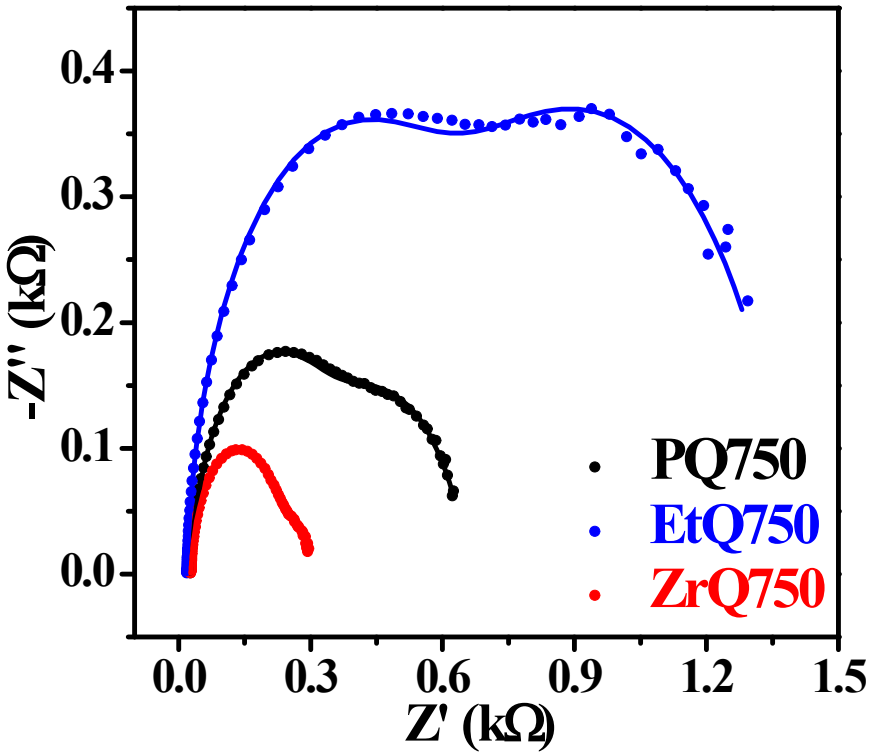

Fig. S20. EIS plots for PQ750, EtQ750, and ZrQ750 photoanodes measured under one sun illumination at 1.23 V *vs.* RHE.

References

[1] Y. Zhu, Q. Qian, G. Fan, Z. Zhu, X. Wang, Z. Li and Z. Zou, *Chinese Chem. Lett.*, 2018, **29,** 791-794.

[2] S. Y. Chae, G. Rahman and O. S. Joo, *Electrochim. Acta,* 2019, **297,** 784-793.

[3] T. T. Hien, N. D. Quang, N. M. Hung, H. Yang, N. D. Chinh, S. Hong, N. M. Hieu, S. Majumder, C. Kim and D. Kim, *J. Electrochem. Soc.*, 2019, **166,** H743-H749.

[4] Y. Fu, C. L. Dong, Z. Zhou, W. Y. Lee, J. Chen, P. Guo, L. Zhao, and S. Shen, *Phys Chem Chem Phys.,* 2016, **18,** 3846-3853.

[5] X. Yang, R. Liu, Y. Lei, P. Li, K. Wang, Z. Zheng and D. Wang, *Appl. Mater. Interfaces*, 2016, **8,** 16476–16485.

[6] J. R. Lakowicz, Principles of fluorescence spectroscopy, Springer, New York, 2006.